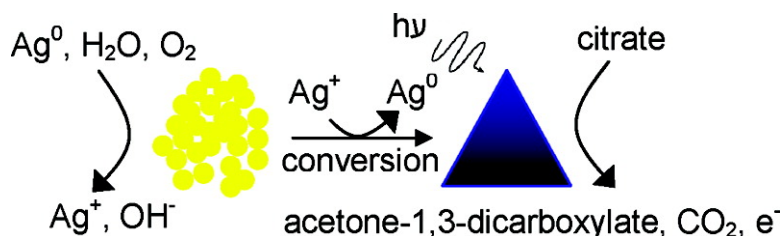Article

Photovoltage Mechanism for Room Light Conversion of Citrate Stabilized Silver Nanocrystal Seeds to Large Nanoprisms

Xiaomu Wu, Peter L. Redmond, Haitao Liu, Yihui Chen, Michael Steigerwald, and Louis Brus

More About This Article

Additional resources and features associated with this article are available within the HTML version:

- Supporting Information
- Links to the 1 articles that cite this article, as of the time of this article download
- Access to high resolution figures
- Links to articles and content related to this article
- Copyright permission to reproduce figures and/or text from this article

View the Full Text HTML

Photovoltage Mechanism for Room Light Conversion of Citrate Stabilized Silver Nanocrystal Seeds to Large Nanoprisms

Xiaomu Wu,* Peter L. Redmond, Haitao Liu, Yihui Chen, Michael Steigerwald, and
Louis Brus

Chemistry Department, Columbia University, New York, New York 10027

Received March 17, 2008; E-mail: xw2130@columbia.edu

Abstract: We investigate the photoconversion of aqueous 8 nm Ag nanocrystal seeds into 70 nm single crystal plate nanoprisms. The process relies on the excitation of Ag surface plasmons. The process requires dioxygen, and the transformation rate is first-order in seed concentration. Although citrate is necessary for the conversion, and is consumed, the transformation rate is independent of citrate concentration. We propose a mechanism that accounts for these features by coupling the oxidative etching of the seed and the subsequent photoreduction of aqueous Ag^+. The reduced Ag deposits onto a Ag prism of specific size that has a cathodic photovoltage resulting from plasmon "hot hole" citrate photo-oxidation. This photovoltage mechanism also explains recent experimental results involving single and dual wavelength irradiation and the core/shell synthesis of Ag layers on Au seeds.

Introduction

The low light intensity photocatalyzed conversion of aqueous colloidal Ag 8 nm round seeds into 30 to 70 nm single crystal disk prisms is very unusual.[1–13] The seeds are initially stabilized by the double layer potential resulting from adsorption of citrate anions on the Ag particle surface. The photoprocess involves surface plasmon excitation, and this feature allows one to tailor the size and shape of the disks by simply varying the irradiation wavelength. Jin et al.[1] first demonstrated the conversion of ~8 nm silver nanospheres passivated by citrate and a coligand bis(*p*-sulfonatophenyl) phenylphosphine dihydrate dipotassium (BSPP) into ~100 nm nanoprisms with normal room light. Dual-beam illumination[2] generated either one or two discrete prism sizes, depending upon choice of wavelengths. The mechanism has been discussed in terms of the charge distribution on the smaller prisms and optically induced force between particles.[2,12,14,15]

The influence of different types of ligands,[3,5] excitation wavelength,[3,4,7,13] laser intensity,[6] pH,[12] and chloride ions[9] have been studied. While all this exploratory work has contributed valuable data and insight, the basic photochemical process remains uncertain.[3,5,7]

Dissolved oxygen is necessary for photoconversion.[3] There may be some sort of Ostwald ripening, with aqueous Ag^+ created by oxidation of metallic Ag by O_2 as previously suggested.[4,16,17] There is ample precedent for oxidative etching in Ag colloidal systems.[18–20] A somewhat related photoprocess[9] is thought to occur by Cl^- assisted oxidative etching of silver nanoparticles, followed by photoreduction of the silver ions produced. Note that chloride is present in neither our photoconversion experiments nor the original report by Jin et al.[1]

Citrate stabilization is necessary for photoconversion of seeds into prisms.[5] In separate experiments we discovered that visible plasmon irradiation of citrate stabilized Ag nanocrystals creates negative photovoltage on the nanocrystal.[21,22] This results from irreversible citrate photo-oxidation by Ag plasmon "hot holes".[4,21] Such cathodic photovoltage greatly enhances the rate of deposition of aqueous Ag^+ onto the Ag nanocrystal.

(1) Jin, R. C.; Cao, Y. W.; Mirkin, C. A.; Kelly, K. L.; Schatz, G. C.; Zheng, J. G. *Science* **2001**, *294*, 1901–1903.
(2) Jin, R. C.; Cao, Y. C.; Hao, E. C.; Métraux, G. S.; Schatz, G. C.; Mirkin, C. A. *Nature* **2003**, *425*, 487–490.
(3) Callegari, A.; Tonti, D.; Chergui, M. *Nano Lett.* **2003**, *3*, 1565–1568.
(4) Maillard, M.; Huang, P. R.; Brus, L. *Nano Lett.* **2003**, *3*, 1611–1615.
(5) Sun, Y. A.; Xia, Y. N. *Adv. Mater.* **2003**, *15*, 695–699.
(6) Tsuji, T.; Higuchi, T.; Tsuji, M. *Chem. Lett.* **2005**, *34*, 476–477.
(7) Bastys, V.; Pastoriza-Santos, I.; Rodriguez-Gonzalez, B.; Vaisnoras, R.; Liz-Marzan, L. M. *Adv. Funct. Mater.* **2006**, *16*, 766–773.
(8) Tian, X.; Chen, K.; Cao, G. *Mater. Lett.* **2006**, *60*, 828–830.
(9) Tsuji, T.; Okazaki, Y.; Higuchi, T.; Tsuji, M. *J. Photochem. Photobiol., A* **2006**, *183*, 297–303.
(10) Jia, H. X. W.; An, J.; Li, D.; Zhao, B. *Spectrochim. Acta, Part A* **2006**, *64*, 956–960.
(11) Jia, H.; Zeng, J.; Song, W.; An, J.; Zhao, B. *Thin Solid Films* **2006**, *496*, 281–287.
(12) Xue, C.; Mirkin, C. A. *Angew. Chem., Int. Ed.* **2007**, *46*, 2036–2038.
(13) Zheng, X.; Xu, W.; Corredor, C.; Xu, S.; An, J.; Zhao, B.; Lombardi, J. R. *J. Phys. Chem. C* **2007**, *111*, 14962–14967.
(14) Hallock, A. J.; Redmond, P. L.; Brus, L. E. *Proc. Natl. Acad. Sci. U.S.A.* **2005**, *102*, 1280–1284.
(15) Wong, V.; Ratner, M. A. *J. Opt. Soc. Am. B: Opt. Phys.* **2007**, *24*, 106–112.
(16) Métraux, G. S.; Jin, R. C.; Mirkin, C. A. *Small* **2006**, *2*, 1335–1339.
(17) Xue, C.; Millstone, J.; Li, S.; Mirkin, C. A. *Angew. Chem., Int. Ed.* **2007**, *46*, 8436–8439.
(18) Lok, C.-N.; Ho, C.-M.; Chen, R.; He, Q.-Y.; Yu, W.-Y.; Sun, H.; Tam Paul, K.-H.; Chiu, J.-F.; Che, C.-M. *J. Biol. Inorg. Chem.* **2007**, *12*, 527–534.
(19) Wiley, B.; Herricks, T.; Sun, Y. G.; Xia, Y. N. *Nano Lett.* **2004**, *4*, 2057–2057.
(20) Henglein, A.; Mulvaney, P.; Linnert, T. *Faraday Discuss.* **1991**, *31*–44.
(21) Redmond, P. L.; Wu, X. M.; Brus, L. *J. Phys. Chem. C* **2007**, *111*, 8942–8947.
(22) Redmond, P. L.; Brus, L. E. *J. Phys. Chem. C* **2007**, *111*, 14849–14854.

Both an oxidizing agent, O_2, and a reducing agent, citrate, are required in this photoripening of seeds, yet no added aqueous Ag^+ is required. One might imagine that a small aqueous Ag^+ equilibrium concentration, due to oxidative seed etching, could be selectively reduced onto nanocrystal prisms with high photovoltage. We previously showed that disk prisms do indeed grow under plasmon irradiation in the presence of millimolar concentrations of Ag^+.[4]

We now quantify this photovoltage mechanism. We experimentally demonstrate that citrate is directly consumed as the photoreaction proceeds. We suggest that the plasmon dephases on citrate covered surfaces, causing photo-oxidation of citrate and creating photovoltage, as well as decreasing the rate of Rayleigh plasmon scattering. The process is first-order in seed concentration and independent of citrate concentration above ~0.5 mM. The rate becomes sublinear in light intensity above ~50 mwatt/cm^2. At low light intensity there is a slow reversible Ostwald-ripening-like transfer of Ag^+ from a large number of small round seeds to a small number of prism nanocrystals having larger photovoltage. Hydroxide simultaneously is produced by reaction of dissolved O_2 on the seed surfaces. Larger photovoltage occurs on specific nanocrystal shapes owing to the well-known relationship between plasmon resonance wavelength and shape. This photovoltage mechanism explains previously reported single and dual beam experiments and growth of Ag shells on Au nanocrystals.

Experimental Section

We explore and simplify the original room light experiment.[2] A "standard" seed solution was synthesized by reducing aqueous $AgNO_3$ (0.091 mM) with $NaBH_4$ (5.46 mM) in the presence of sodium citrate (Na_3cit, 0.27 mM) (see Supporting Information). The resulting colloid was aged overnight under stirring in the dark (evolution in the UV spectra shown in Figure S1). TEM analysis showed that the round seeds were typically 8–10 nm in diameter with a wide distribution. The solution was then irradiated in 10 mm plastic cuvettes between two conventional fluorescence tubes (F15T8/CW 15W, Cool White, spectrum shown in Figure S2) in a light box at 43 °C for 2–4 h. The intensity is ~4 mwatts/cm^2 incident on both cuvette sides facing the lamps. The natural solution pH is initially ~9.3 without buffer and usually goes up to 9.5 at the end of the conversion. Some experiments were conducted with different lines of an unpolarized Ar^+ ion laser with a spot size of 12 cm^2 covering one cuvette face. To simplify the mechanism, we only use citrate stabilization, in contrast to the experiments of Jin et al.[2] that used combinations of citrate and BSPP. As previously reported,[2,5] seed samples prepared using only citrate have a broader size distribution and are not completely transformed into nanoprisms under visible light irradiation. The lack of a costabilizer also resulted in a wider size distribution of the prisms formed.

The photochemical process has been characterized by UV–vis spectroscopy (Hewlett-Packard 8453), TEM (JEOL JEM-100CX), ^{1}H NMR (Bruker 500 MHz), and Light Scattering (Malvern Zetasizer Nano-ZS). NMR provides information about the change in aqueous (nonadsorbed) citrate concentration during the conversion. For NMR we prepared and irradiated the seeds in deuterium oxide (D_2O) and then added dioxane as the internal standard before taking spectra. All the other reaction conditions were kept the same as previously described. As a control, the conversion rate and yield were unaffected in D_2O compared to H_2O.

The Light Scattering instrument measures the *in situ* zeta potential and size distribution of the colloidal nanoparticles through means of electrophoretic and dynamic light scattering.[23,24] The zeta
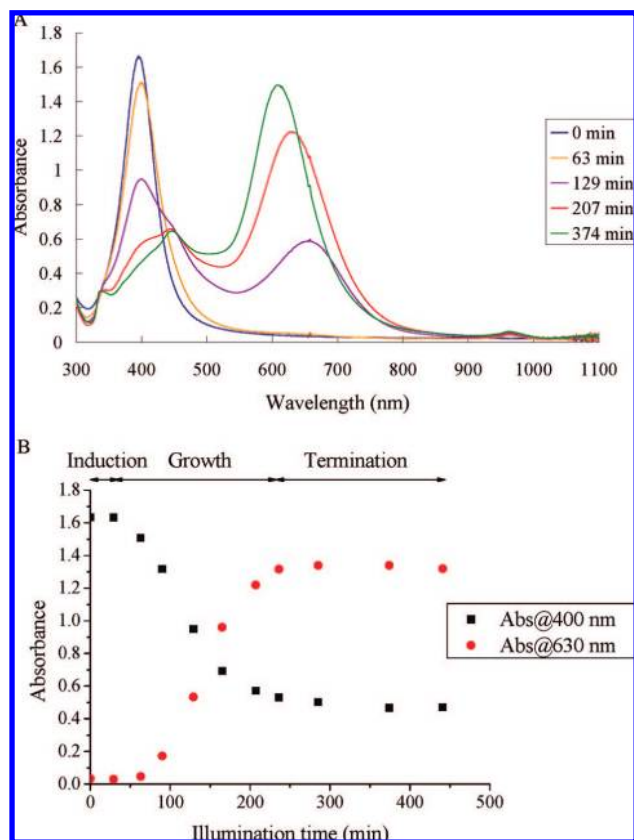

Figure 1. (A) UV–vis spectra of the colloid taken after 0, 63, 129, 207, 236, and 374 min of white light illumination. (B) Corresponding absorbance at 400 nm (black square, λ_{max} for the starting Ag seeds) and 630 nm (red diamond, λ_{max} for in-plane dipole bands of the nanoprisms) as a function of illumination time.

potential relates to the electrostatic potential generated by the electrical double layer at the surface of a colloidal particle, comprising the ion fixed Stern layer and diffuse layer. A greater absolute value predicts a higher stability of the colloidal suspensions.[25–28] Possible aggregation causes a change in particle zeta potential and size and can be evaluated *in situ*.

Results and Discussion

Kinetic Analysis. Figure 1 shows the UV–vis spectral evolution for standard seeds, similar to that previously reported. The peak at 400 nm is characteristic for round seeds, whereas the peak at 630 nm corresponded to the in-plane dipole bands of the nanoprisms.[1,2,29] Three approximate stages can be identified in both the decay of the seeds and the appearance of the disk prisms: induction (0–50 min), growth (50–250 min), and completion (>250 min). During the induction period, the peak at 400 nm shifts slightly to the red, probably due to the formation of oblong particles or small aggregates.[29–31] During

(23) Magdassi, S.; Bassa, A.; Vinetsky, Y.; Kamyshny, A. *Chem. Mater.* **2003**, *15*, 2208–2217.

(24) Faulds, K.; Littleford, R. E.; Graham, D.; Dent, G.; Smith, W. E. *Anal. Chem.* **2004**, *76*, 592–598.

(25) Bastos, D.; Nieves, F. J. D. *Colloid Polym. Sci.* **1994**, *272*, 592–597.

(26) Puertas, A. M.; de las Nieves, F. J. *J. Colloid Interface Sci.* **1999**, *216*, 221–229.

(27) Evans, D. F. W. H. *The colloidal domain: where physics, chemistry, and biology meet*, 2nd ed.; Wiley-VCH: New York, 1999.

(28) Ishikawa, Y.; Katoh, Y.; Ohshima, H. *Colloids Surf., B* **2005**, *42*, 53–58.

(29) Kelly, K. L.; Coronado, E.; Zhao, L. L.; Schatz, G. C. *J. Phys. Chem. B* **2003**, *107*, 668–677.

(30) Jensen, T.; Kelly, L.; Lazarides, A.; Schatz, G. C. *J. Cluster Sci.* **1999**, *10*, 295–317.
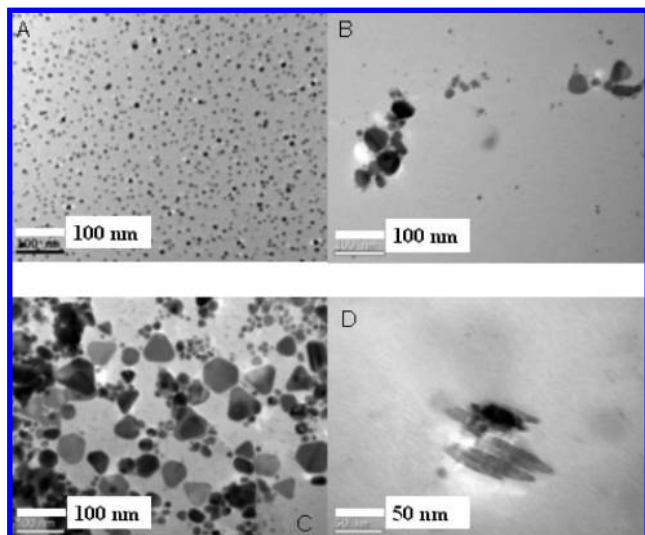
Figure 2. TEM images of the nanoparticles after (A) 0, (B) 43, and (C) 300 min of white light irradiation. (D) Thickness of the prism is shown to be ~10 nm.
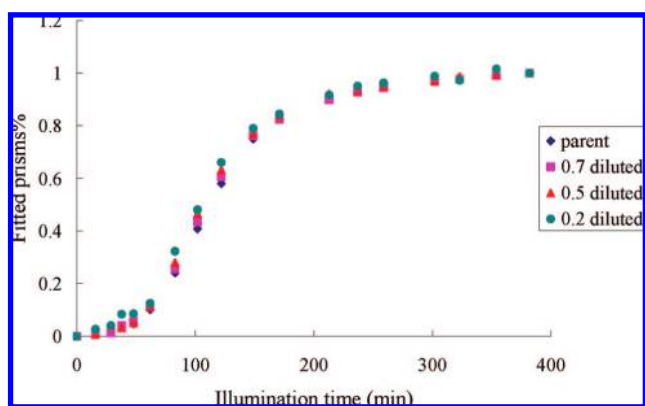

Figure 3. Plot of fitted prisms% vs illumination time under fluorescence lamp illumination for parent, 0.7 (dilution factor), 0.5, and 0.2 diluted "standard" seeds solutions.

the growth phase a quasi-isosbestic point occurs at approximately 450 nm as previously observed;[7] this indicates that the concentration of any intermediates is never very high. The blue shift of the in-plane dipole bands of the prisms at ~630 nm near the end of the conversion was attributed the roundness of the tips on the triangles.[1] In Figure 2 TEM images show that some small nanoprisms are present in the induction period. Both round and triangular highly crystalline final disks are observed. Triangular edge lengths are in the 30−70 nm range, with a thickness of ~10 nm. Some seeds remain in the final product.

The quasi-isobestic point in the spectra allows us to quantify the kinetics by fitting the spectra in time as linear combinations of the initial seed spectrum, and the final spectrum, which is predominately prisms with a some unreacted seeds. We then estimated the percentage of seeds and prisms by linear least-squares regression. Figure 3 shows the evolution of the fitted prism percentage, which shows sigmoidal autocatalytic (initiation-growth-completion) kinetics.

The Ag mass from ~30 seeds must combine to make one prism. If seeds move independently in solution and fusion of touching seeds creates prisms, a complex kinetic order in seed
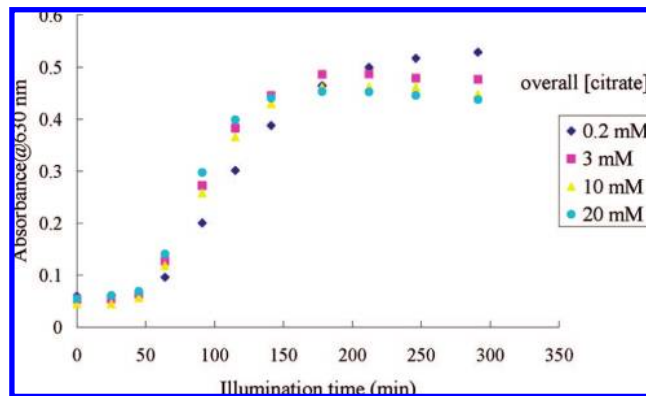

Figure 4. Absorbance at 630 nm of the colloid solutions vs illumination time. The overall [Na₃cit] is 0.2, 3, 10, 20, and 30 mM. Seed concentration was kept constant in all the samples.

concentration should be observed. To test this, the standard seed solution was diluted with aqueous sodium citrate and KNO_3 solutions to keep both the citrate concentration and ionic strength constant. We find first-order autocatalytic kinetics in all stages of the reaction, even when the seed concentration is diluted by a factor of 5. That is, for different seed concentrations, the time dependent optical density can be represented as $OD(t) = OD(t = 0) \times F(t)$, where the sigmoid autocatalytic function $F(t)$ is independent of seed concentration. This is shown in Figure 3 where the kinetic traces have been rescaled to normalize initial OD. Assuming that the spectra in the beginning and at the end are pure spectra of the seeds and prisms, respectively, and the intermediate ones are the linear combinations of the two, we hereby calculate seeds% and prisms% through least-squares regression. Other aqueous salt diluents such as $Na_2B_4O_7$ were also tested, with essentially the same results. This result argues against direct fusion of seeds.

Prisms do not flocculate as growth occurs. The colloid is stabilized by electrostatic double layers resulting from citrate anion adsorption. The seed solution is indefinitely stable at 23 °C in the dark. Such electrostatic stabilization should be reduced at high salt concentration as the Debye length shortens. The calculated initial aqueous salt concentration 7.2 mM is established by the oxidation products of the reducing agent $NaBH_4$; only 1.6 mM of this 7.2 mM is sodium citrate. We observed that if the salt concentration is raised above ~21.0 mM by addition of KNO_3, the seeds coagulate and settle to the bottom. In the limited ionic strength range up to 21.0 mM, the parent seed colloid photoconversion yield and rate are almost unchanged.

There is a dynamic equilibrium between aqueous citrate and citrate strongly adsorbed on Ag. Many groups[32–35] have studied the aggregation kinetics of aqueous Ag colloids, which in general is highly dependent on the ligand species and concentration. The seed solution in the dark was stable for citrate concentrations from 0.27 mM to 30 mM for [initial $NaBH_4$] = 5.45 mM. Figure 4 shows that the photoconversion kinetics and yield are essentially unchanged in the range 0.27 to 20 mM citrate concentration; here extra citrate was added to a standard seed solution after overnight aging. These results imply that

(31) Hao, E.; Schatz, G. C. *J. Chem. Phys.* **2004**, *120*, 357–366.

(32) Dagastine, R. R.; Grieser, F. *Langmuir* **2004**, *20*, 6742–6747.
(33) Moskovits, M.; Vlckova, B. *J. Phys. Chem. B* **2005**, *109*, 14755–14758.
(34) Van Hyning, D. L.; Klemperer, W. G.; Zukoski, C. F. *Langmuir* **2001**, *17*, 3128–3135.
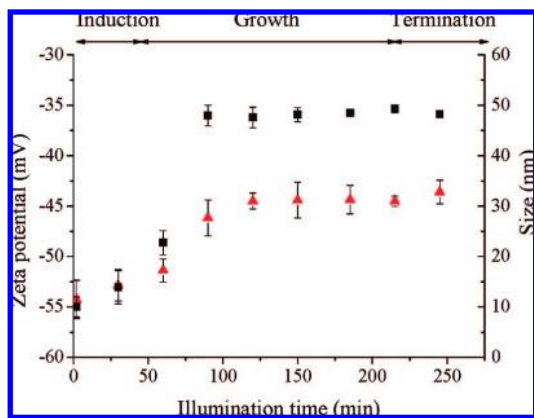(35) Van Hyning, D. L.; Zukoski, C. F. *Langmuir* **1998**, *14*, 7034–7046.

Figure 5. Evolution of the Zeta potential (red triangle) and size (black square) of the nanoparticles as a function of illumination time. The error bars were calculated from five repeated measurements.

Figure 6. Change in the absorbance at 630 nm (black square, λ_{max} for in-plane dipole bands of the nanoprisms) and citrate concentration (red triangle) as a function of illumination time.

above 0.27 mM we have a complete citrate monolayer on the seeds; a similar conclusion was reached earlier in the direct measurement of photovoltage.[21] If less citrate was present in the initial seed synthesis, then seeds showed aggregated TEM images, and photoconversion was slower with depressed yields. If the citrate concentration was lower than 0.09 mM, the optical spectra indicated essentially no prism photoformation. This confirms the conclusion reached by Xia et al. that citrate is essential.[5] In the 20−40 mM citrate range, the photoconversion yield was decreased, and above 40 mM the high ionic strength caused precipitation as illumination occurred. Note that 30 mM citrate does not coagulate the seeds despite the very high ionic strength, unlike the situation with added KNO_3.

The commercial Zetasizer Light Scattering instrument uses a proprietary analysis (not corrected for shape) to convert electrophoretic and dynamic light scattering data into zeta potential and size. The 633 nm scattering laser is resonant with the product disk prisms but not the initial seeds. In Figure 5, as disk prisms are formed, the zeta potential shifts slightly from −55 to −45 mV. Both initial and final values imply good electrostatic stabilization, consistent with the absence of precipitation. The Zetasizer dominant size measurement shows growth from seeds to disk prisms, consistent with the TEM results.

The apparent zeta potential is more positive for the prisms, which might suggest loss of citrate as photoconversion proceeds. As previously mentioned, we have proposed that unrelaxed, ballistic "hot holes" created in Ag plasmon excitation oxidize adsorbed citrate molecules into acetone-1,3-dicarboxylate, which is unstable and simultaneously decarboxylates to form acetyl acidic acid and acetone.[36] The resulting Ag cathodic photovoltage, but not the loss of citrate itself, was directly measured.[21] We now use NMR to probe the aqueous citrate concentration, which should be in dynamic equilibrium with adsorbed citrate. As shown in Figure 6, the aqueous citrate concentration drops from 0.25 mM to 0.13 mM during photoconversion over 5 h. Control experiments showed that the citrate concentration stayed constant if the colloid solution was kept in the dark or if no nanoparticles were present in a pure aqueous solution of sodium citrate. The NMR does not directly observe adsorbed citrate. With simple calculations of the volumes, surface areas, and concentrations of the seeds and prisms, and assuming complete
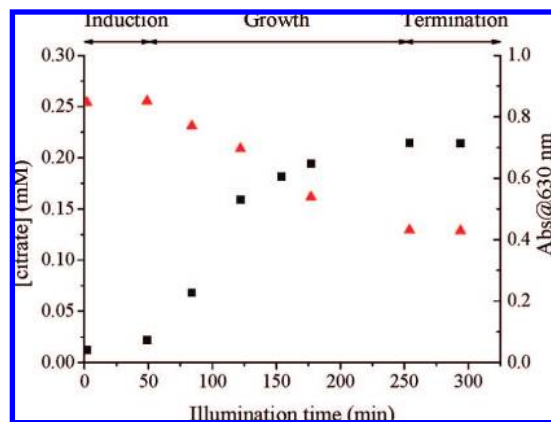
coverage with a surface area required for each citrate molecule of 0.25 nm^2,[32] we estimate the equivalent adsorbed citrate concentration to be 0.005 mM on the initial seeds and 0.002 mM on the final prisms, which have less total surface area. Summing adsorbed and aqueous citrate, we have 0.26 and 0.13 mM total citrate before and after the conversion, respectively, which agrees well with the actual starting citrate concentration 0.27 mM in the seed preparation. Thus citrate is consumed, but at 0.27 mM initial concentration, enough aqueous citrate remains to ensure disk adsorption and stability. In D_2O, only citrate peaks were observed. Presumably, the $-CH_2-$ protons of acetone-1,3-dicarboxylate are acidic enough to exchange with D_2O. Indeed, with a water suppression technique, we saw additional peaks that can be assigned to acetone-1,3-dicarboxylate, acetyl acidic acid, and acetone after the "standard" aqueous seeds solution was irradiated for 4 h.

All experiments above were done with the "Cool White" fluorescent lamps, which have a broad visible spectrum that excites the plasmons of seeds, possible intermediates, and triangular disks. We compared this with illumination at the fixed Ar^+ laser wavelengths 458 and 514 nm. The blue 458 nm line has the greater overlap with the seed plasmon spectrum. The product formed under 458 nm excitation shows a prism plasmon at 485 nm; that formed under 514 nm irradiation shows a prism plasmon at 580 nm. At 514 nm prisms with an average edge length of ∼40 nm were formed. Larger disk prisms grow for longer wavelength excitation, consistent with earlier studies. In Figure 7 the fitted prism percentage for 458 nm excitation shows fast growth with almost no induction period. Under the same 10 mwatt/cm^2 intensity but at longer 514 nm wavelength, growth is much slower; it is similar to that with the fluorescent lamps. In Figure 8 the 514 nm prism spectra exhibited two additional broad peaks located at 810 and 960 nm. These peaks can be attributed to the existence of larger prisms or to prism aggregation that induces a strong coupling between individual prisms.[2,31,37]

Is this photoconversion process simply proportional to cumulative irradiation fluence? The effect of illumination intensity was tested using the 514 nm laser line. Figure 9 compares spectra taken at different powers for constant fluence. Below ∼10 mwatts/cm^2, the spectra are about the same; the process is linear. When the laser power intensity was reduced

(36) Munro, C. H.; Smith, W. E.; Garner, M.; Clarkson, J.; White, P. C. *Langmuir* **1995**, *11*, 3712–3720.

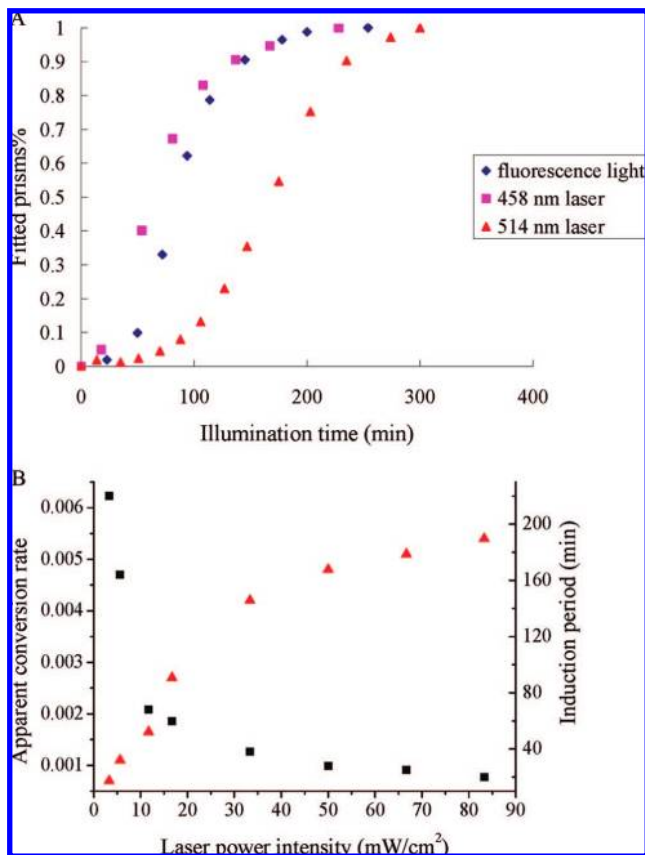(37) Sun, Y. G.; Mayers, B.; Xia, Y. N. *Nano Lett.* **2003**, *3*, 675–679.

Figure 7. (A) Fitted prisms% vs illumination time under Ar-ion laser at 458 and 514 nm (10 mW/cm^2). The optical density of the initial seeds spectrum at 458 and 514 nm are 0.25 and 0.14, respectively. Such a difference gives rise to the distinct conversion kinetics. (B) Plot of the apparent conversion rate (red triangle) and induction period (black square) vs power intensity of the 514 nm laser. (Same batch of seeds were used; the apparent conversion rate was calculated from the slope ($\Delta A/\Delta t$) of the linear growth section of the absorbance at 630 nm vs time curve as shown in Figure 1B).

to ca. 2 mwatts/cm^2, the seed spectrum did not change over a period of 8 h. The reaction is so slow that we can not measure the kinetics. Above ~10 mwatts/cm^2, the process starts to be sublinear; the conversion percentage decreases at higher intensities. In Figure 10 we weight the time axis to compensate for different intensities. If the process was strictly proportional to fluence, then all disk growth curves would superimpose. Instead there is a significant sublinearity of the growth rate of fitted prism percentage at 50 and 83 mwatts/cm^2 (also shown in Figure 7B). Linear behavior indicates that there is a slow, rate-limiting photochemical process at low intensity. Sublinear behavior at higher intensities implies that some constant rate thermal process has become rate-limiting as the photochemical process speeds up. We conclude the growth process includes at least two fundamental steps, one photochemical and one thermal.

Chemical Reactions and Mechanism. The photochemical process occurs at very low light intensity, a small fraction of solar intensity, over a period of hours or days. The intensity is too low for mechanisms involving optical forces[14,15] or light induced thermal heating.[38] We propose that the mechanism is a combination of oxidative etching of reduced Ag, followed by reduction of Ag$^+$ on prisms, which have built up a photovoltage due to citrate photooxidation:

(38) Redmond, P. L.; Walter, E. C.; Brus, L. E. *J. Phys. Chem. B* **2006**, *110*, 25158–25162.
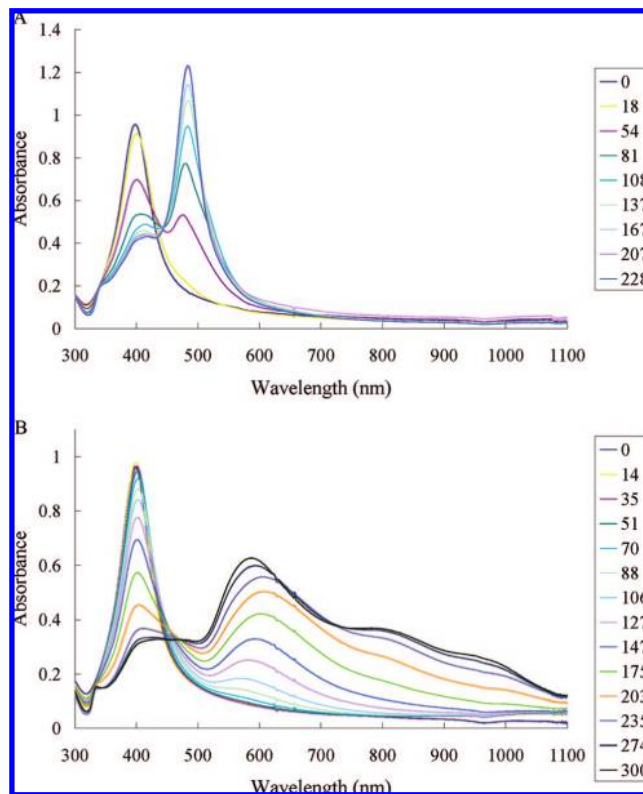
Figure 8. (A) UV−vis spectra of the colloid taken after 0, 18, 54, 81, 108, 137, 167, 207, and 228 min of illumination with Ar-ion laser at 458 nm, 10 mW/cm^2. (B) UV−vis spectra of the colloid taken after 0, 70, 106, 147, 203, 235, 300, 370, and 459 min of illumination with Ar-ion laser at 514 nm, 10 mW/cm^2.
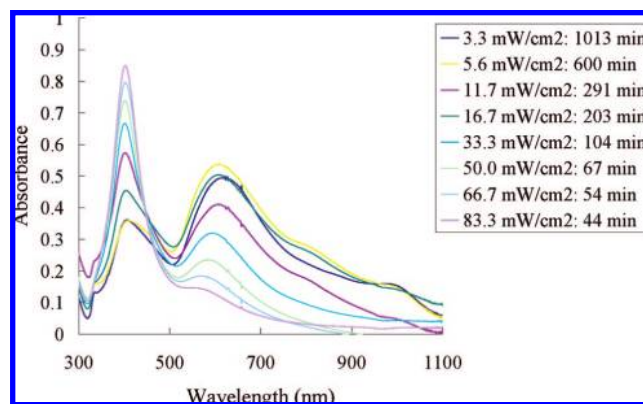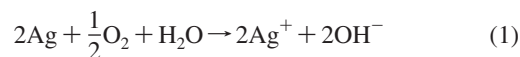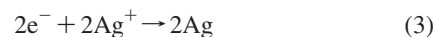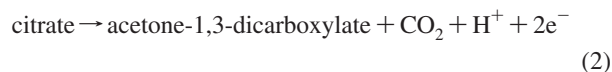

Figure 9. Spectra under the same flux at different intensities.

Seeds that absorb/scatter light weakly reduce dioxygen and lose Ag$^+$:

$$2Ag + \frac{1}{2}O_2 + H_2O \rightarrow 2Ag^+ + 2OH^- \qquad (1)$$

Prisms that absorb/scatter more strongly oxidize citrate, reduce Ag$^+$, and gain Ag:

$$citrate \rightarrow acetone\text{-}1,3\text{-}dicarboxylate + CO_2 + H^+ + 2e^- \qquad (2)$$

$$2e^- + 2Ag^+ \rightarrow 2Ag \qquad (3)$$

The overall reaction is the indirect photo-oxidation of citrate by O$_2$, catalyzed by silver:

$$citrate + \frac{1}{2}O_2 \rightarrow acetone\text{-}1,3\text{-}dicarboxylate + CO_2 + OH^-$$

$$(4)$$
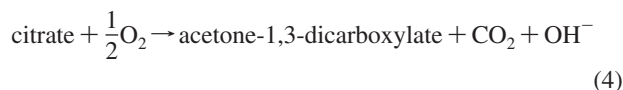
In the absence of seeds, solutions of Ag^+ and citrate show no reaction at 23 °C in equilibrium with air. 0.5 equiv of citrate is required to reduce 1 equiv of Ag^+ onto the growing Ag disk, while our NMR analysis shows that $\sim$1.5 equiv of citrate are consumed during the photoconversion process. The electrons donated by the excess citrate might be consumed by reaction with a proton or O_2.

Oxidation of Metallic Ag. There is ample precedent for oxidative etching producing a low equilibrium $[Ag^+]$. By direct Ag electrode measurement we establish an upper limit of 1 μM for $[Ag^+]$ in the seed solution. Very recently Lok et al. measured $\sim$0.1 μM of aqueous Ag^+ after bubbling O_2 through a solution of freshly prepared Ag nanocrystals.[18] The experimental effect of oxygen pressure,[3,16] pH,[12] and additives[12] are consistent with the expected behavior of the O_2 and Ag redox potentials. Under an inert atmosphere, no reaction takes place. The effect of increasing aqueous $[O_2]$, or adding other oxidizing agents, on accelerating the conversion was previously reported.[3,16] The solution pH increased from 9.3 to 9.5 after the photoconversion process. In neutral or acidic seed solution, prism formation does not occur. Either an initial pH value above 12, or adding Cl^- ions to the solution, experimentally stops the conversion, as $[Ag^+]$ is lower due to the formation of AgOH and AgCl, respectively.

Photo-oxidation of Citrate. Adsorbed citrate ions undergo photoassisted oxidation, injecting electrons into the silver nanocrystal (eq 2) and creating a cathodic photovoltage as previously measured.[21] Photo-oxidation of adsorbed citrate is a new surface-induced plasmon decay channel and presumably decreases the Rayleigh scattering rate and local field enhancement. Munro et al.[36] suggested two of the three citrate carboxylic groups bond to the Ag surface. Citrate undergoes both thermal (at high temperature) and plasmon induced photo-oxidation.[21,39,40]

Growth and Shape Evolution. Different Ag nanocrystals will develop different photovoltages depending upon how strongly they interact with the light. For example, round seed nanocrystals with a plasmon at an $\sim$400 nm wavelength interact only weakly with the 514 nm Ar^+ laser line. A small fraction of rod- or prism-shaped seeds will interact resonantly at the laser line. Growth is also favored in crystalline as opposed to amorphous particles of the correct shape. This small fraction will develop a larger (more negative) photovoltage and grow. The growth rate will be first-order in seed concentration as these minority rod- and prism-shaped seeds are diluted.

There should be two kinetic regimes depending upon whether the Ag^+ disk photoreduction rate is large or small with respect to both the Ag^+ mass transfer rate onto the disk surface and the seed oxidation rate. In the limit of low light intensity, photoreduction will be slower and likely rate-limiting. In this limit, the photochemical process does not significantly change the $[Ag^+]$ established by initial thermodynamic equilibrium; the concentration of Ag^+ will be constant as long as some reduced Ag seeds remain. Seeds will slowly dissolve as prisms grow. The steady state prism cathodic photovoltage corresponds to an expected lower "thermodynamic" $[Ag^+]$ at the prism surfaces.
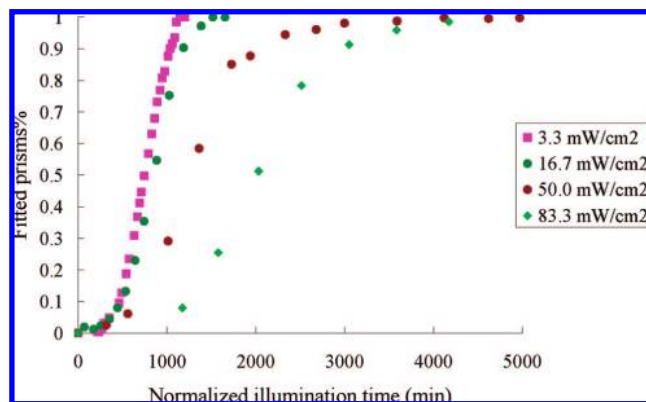

Figure 10. Fitted prisms% vs illumination time normalized by laser intensities.

This is a light driven Ostwald ripening process, somewhat analogous to the nonphotochemical Ag Ostwald ripening, in which Ag mass shifts in response to the size dependence of the Ag electrochemical redox potential.[41,42] The rate is independent of the concentration of aqueous citrate because there is a complete adsorbed layer for the concentration range studied. The photovoltage is an increase in the double layer voltage. An electron on the nanocrystal tunnels across the double layer to reduce Ag^+. The reduction rate grows exponentially with increasing photovoltage.[22]

The product adopts a prism plate morphology. Prisms are also observed in purely thermal Ag seed growth processes involving surfactants that selectively adsorb on certain crystal planes, thus inducing anisotropic growth.[37,43–48] Citrate likely causes prism growth by adsorbing more strongly to the top and bottom (111) planes.[5,37,48] The lateral prism size is controlled by the irradiation wavelength. The in-plane plasmon peak red-shifts as a disk grows. As this peak approaches 514 nm (for example) from the blue, the light interaction cross section and the net rate of Ag^+ reduction increase, thus accelerating the growth rate. The process thus is autocatalytic as observed. However, when the plasmon peak shifts to the red of 514 nm, the net light interaction decreases. Growth stops because disks with resonant lateral size now have a more negative photovoltage.

At low intensity there is reversible disk growth, with the net rate of Ag transfer from seeds to prisms being slower than the rates of oxidative etching and diffusion. This gives some insight into why the product prisms are such perfect single crystals.[1] Guertierrez and Henglein demonstrated in 1993 that reversible reduction processes make highly crystalline Ag particles that have unusually narrow plasmon resonances.[49] Contrast this with the initial relatively fast borohydride reduction process, which makes low quality Ag seeds. Note also that photovoltage will be higher on crystalline particles, which have slower internal electron relaxation rates than amorphous particles.

(39) Sato, T.; Kuroda, S.; Takami, A.; Yonezawa, Y.; Hada, H. *Appl. Organomet. Chem.* **1991**, *5*, 261–268.

(40) Rogach, A. L.; Shevchenko, G. P.; Afanaseva, Z. M.; Sviridov, V. V. *J. Phys. Chem. B* **1997**, *101*, 8129–8132.

(41) Chaki, N. K.; Sharma, J.; Mandle, A. B.; Mulla, I. S.; Pasricha, R.; Vijayamohanan, K. *Phys. Chem. Chem. Phys.* **2004**, *6*, 1304–1309.

(42) Redmond, P. L.; Hallock, A. J.; Brus, L. E. *Nano Lett.* **2005**, *5*, 131–135.

(43) Chen, S. H.; Carroll, D. L. *Nano Lett.* **2002**, *2*, 1003–1007.

(44) Pastoriza-Santos, I.; Liz-Marzan, L. M. *Nano Lett.* **2002**, *2*, 903–905.

(45) Pillai, Z. S.; Kamat, P. V. *J. Phys. Chem. B* **2004**, *108*, 945–951.

(46) Yamamoto, T.; Yin, H. B.; Wada, Y.; Kitamura, T.; Sakata, T.; Mori, H.; Yanagida, S. *Bull. Chem. Soc. Jpn.* **2004**, *77*, 757–761.

(47) Deivaraj, T. C.; Lala, N. L.; Lee, J. Y. *J. Colloid Interface Sci.* **2005**, *289*, 402–409.

(48) Métraux, G. S.; Mirkin, C. A. *Adv. Mater.* **2005**, *17*, 412–415.

(49) Gutierrez, M.; Henglein, A. *J. Phys. Chem.* **1993**, *97*, 11368–11370.

In the low intensity linear regime, the growth rate is a lower limit for the Ag^+ diffusion mass transfer rate, which varies linearly with $[Ag^+]$. As irradiation intensity increases, the kinetics will enter the second, sublinear regime when the growth rate equals the Ag^+ mass transfer rate. In Figure 7A the time averaged growth rate over 5 h using the 514 nm laser line at 10 mwatts/cm^2 is ~28 silver atoms per prism per second. Experimentally the growth rate becomes sublinear near 50 mwatts/cm^2, where the extrapolated linear growth rate would be ~140 atoms/s. Using Sugimoto's model,[50] we calculate that this growth rate would equal the mass transfer rate if $[Ag^+] \approx 10^{-9}$ M. We approximate the prism as a sphere of radius 13 nm with a Ag^+ diffusion constant in water of 1.65×10^{-5} cm^2/s.[50] Thus, if the equilibrium $[Ag^+]$ is ~10^{-9} M, then the observed sublinear behavior may represent a switch to diffusion limited growth. Direct measurement of $[Ag^+]$ during the growth would be important.

Previously, a direct measurement of photocurrent for adsorbed nanocrystals showed a linear dependence on light intensity at higher $[Ag^+]$; this result suggests the citrate photo-oxidation quantum yield is independent of intensity.[22] The autocatalytic growth rate with the fluorescent lamps is about the same as with the 514 nm laser at 10 mwatts/cm^2. With the lamps we estimate a linearized citrate photo-oxidation rate of 396 molecules per second per growing prism, from the data in Figure 6. In this estimate we neglect photo-oxidation on seeds, so that this number is a upper limit for the linearized, average photo-oxidation rate on prisms. Nevertheless, this estimate is only an order of magnitude above the Ag atom growth rate per prism. Thus the quantum yield of Ag^+ reduction per photoelectron from citrate oxidation, at low light intensity, must be relatively high, even at $[Ag^+] \approx 10^{-9}$ M.

Single and Dual Wavelength Illumination. In the low intensity linear "thermodynamic" regime, the one nanocrystal morphology with the largest cathodic photovoltage will grow at the expense of the others, albeit perhaps only slowly. Lower $[Ag^+]$ or higher light intensity can shift the kinetics into the second regime, in which either seed oxidation or Ag^+ mass transport is rate-limiting. Here we expect less competition between morphologies. In this regime, or at intermediate times at low intensity, several morphologies may grow. Single wavelength 550 nm illumination, as an example, is resonant with both the quadrupole plasmon of ca. 150 nm edge-length disks and dipole plasmon of ca. 70 nm edge-length disks. That there are two discrete disk sizes in a resonance situation is generally true for single visible and near IR wavelengths. Thus bimodal growth is possible for a single fixed wavelength, if two different discrete sizes have a significantly lower photovoltage than other morphologies. Jin et al. have reported growth of two discrete sizes for single wavelength irradiation.[2]

Dual-beam experiments[2] further explore such competing growths. If two different irradiation wavelengths are separately resonant with the quadrapolar and dipolar resonances of one discrete disk size, then that size likely will have a higher photovoltage than other morphologies that have only one resonant plasmon. Here single size growth should occur. Jin et al. observed single size 70 nm edge disk growth for 550/450 nm and 550/340 nm dual beam irradiation. The 550 nm wavelength is resonant with the dipolar plasmon, and 450 and 340 nm coincide with the quadrupole plasmon of a 70 nm disk. In other dual beam experiments where such a double resonance for one size does not occur, bimodal growth was observed with different sizes being favored by each wavelength.

Au Colloidal Photovoltage. Seed-to-prism photoconversion for citrate stabilized Au nanocrystals is not observed.[16] However, photogrowth of an Ag shell on a citrate stabilized, plasmon irradiated Au nanocrystal has been observed, in a system that simultaneously contains small Ag seeds.[17] Ag^+ is created by oxidative etching of Ag seeds. Importantly, this experiment implies that photovoltage does develop on the citrate stabilized Au nanocrystals under plasmon irradiation, leading to reduction of aqueous Ag^+. The main reason Au seeds do not directly photoconvert into Au disk prisms is that the oxidative etching equilibrium concentration of aqueous Au ions is too low, as has been recently proposed from a direct comparison of the Au and Ag redox potentials.[16]

Conclusion

We explore the novel photoconversion of aqueous citrate stabilized silver nanocrystal seeds to disk nanoprisms, using UV−vis spectroscopy, TEM, ^{1}H NMR, and Light Scattering. We propose a mechanism involving citrate photo-oxidation by hot "holes" from plasmon dephasing on the surface, oxidative etching of silver in the presence of O_2, and selective reduction of aqueous silver ions on crystalline disk prisms with larger photovoltage. This mechanism allows us to understand several previously reported experiments.

Note Added in Proof. After this article was accepted for publication, a related mechanistic study appeared: Xue, C.; Métraux, G. S.; Millstone, J. E.; Mirkin, C. A. *J. Am. Chem. Soc.* **2008**, ASAP Article; DOI: 10.1021/ja8005258.

Supporting Information Available: Synthesis of the seed colloid, evolution in the UV−vis spectra, and emission spectrum of the fluorescence lamp. This information is available free of charge via the Internet at http://pubs.acs.org

JA8018669

(50) Furukawa, K.; Takahashi, Y.; Sato, H. *Geochim. Cosmochim. Acta* **2007**, *71*, 4416–4424.